第 28 卷第 11 期 无 机 化 学 学 报 Vol.28 No.11
2012 年 11 月 CHINESE JOURNAL OF INORGANIC CHEMISTRY 2478-2484

球形 V-MCM-48 的简单合成方法

许晓颖 孔 岩* 陈 玉 赵 南 时晓波 王 军
(南京工业大学化学化工学院材料化学工程国家重点实验室,南京 210009)

摘要:活性金属掺杂的具有三维立方孔道结构的 MCM-48 在芳烃的氧化反应具有潜在应用价值。使用乙醇做助溶剂,在低的模板剂浓度下,经过一步水热法首次合成了球形的 V-MCM-48。通过 XRD,场发射扫描电镜,氮气吸附–脱附,红外,拉曼,核磁,X 射线光电子能谱和 ICP 等技术对样品进行了表征。结果表明这些样品具有大的比表面积(1 005 $m^2 \cdot g$),有序的孔道结构。当 V/Si 的物质的量比高达 2.91%时,仍没有出现 V_2O_5 晶体。大部分的钒进入了硅的骨架。所合成材料在低温过氧化氢直接氧化苯乙烯的反应中表现出良好的催化性能。

关键词:介孔;球形形貌;合成;苯乙烯氧化
中图分类号:O643.36+1;O643.36+4;O643.32+2 **文献标识码**:A **文章编号**:1001-4861(2012)11-2478-07

Facile Synthesis of Spherical V-MCM-48

XU Xiao-Ying KONG Yan* CHEN Yu ZHAO Nan SHI Xiao-Bo WANG Jun
(*State Key Laboratory of Materials-Oriented Chemical Engineering, College of Chemistry and Chemical Engineering, Nanjing University of Technology, Nanjing* 210009, *China*)

Abstract: Spherical V-MCM-48 was synthesized by one-step hydrothermal method under low template concentration using ethanol as the co-solvent. The materials were characterized by XRD, FS-SEM, N_2 adsorption, FTIR, Raman, NMR, XPS and ICP. The results show that the materials are with high specific surface area (1005 $m^2 \cdot g^{-1}$), ordered mesoporous structure and spherical morphology. V_2O_5 crystal is not found when the V/Si molar ratio is 2.91%. Most of vanadium is incorporated to the framework of silica. The materials are effective catalysts in the oxidation of the styrene with H_2O_2 under low temperature.

Key words: V-MCM-48; spherical morphology; synthesis; styrene oxidation

Since mesoporous molecular sieves were reported for the first time by Mobil company in 1992 [1-2], they have rapidly become the focus of chemistry and material science because of their high specific surface area, large pore volume, well-ordered pore structure with uniform pore size distribution from 2 to 30 nm. The well-known M41S mesoporous material family contains several unique members: the hexagonal MCM-41, which has attracted special attention due to its potential application as the support for catalysts and as advanced materials [3-5], and cubic MCM-48, which exhibits even more excellent performance than MCM-41 in adsorption and heterogeneous catalysis, due to its three-dimensional interconnected cubic pore structure. Unfortunately, different from MCM-41, MCM-48 can only be prepared in limited conditions. Even minor change in pH value, temperature, aging time and concentration of template may lead to the

收稿日期:2012-02-28。收修改稿日期:2012-05-08。
国家自然科学基金(No.21276125,20876077,20976084 和 21136005)、江苏省自然科学基金支撑计划(BE2008142)和江苏省高校自然科学基金重大项目(10KJA530015)资助项目。
*通讯联系人。E-mail:kongy36@njut.edu.cn

absence of cubic mesoporous structure. Generally, MCM-48 is prepared with organic silicon sources, high concentration of surfactant templates, alkali, and H_2O[6-8]. In previous work, some researchers employed certain special methods to prepare MCM-48 with high quality and good reproducibility. For example, the gemini dicationic surfactants were utilized to synthesize MCM-48 [9-10] with highly improved reproducibility. However, the gemini dicationic surfactants are rather expensive, this limits its industrial application. Moreover, attempts were made to dramatically decrease the amount of surfactant by adding co-solvent into the synthetic solution[11].

Pure silica MCM-48 lacks of necessary active center, which limits its applications in catalytic reaction. To construct catalytic active sites on this mesoporous material, one effective method is to modify the nature of the silica framework by incorporation of heteroatom, however, this may lead to the destruction of mesoporous structure. Therefore, the synthesis of MCM-48 with heteroatom in the framework is a challenge.

Spherical morphology is especially desirable because of its advantages in heterogeneous catalysis, chromatographic separations and controlled delivery[12-15]. Although the study on morphology of pure MCM-48 has been reported [16], researches on the morphology of heteroatom incorporated MCM-48 prepared by conventional hydrothermal synthesis method are scarcely reported because of the limited synthesis method of MCM-48. Therefore, the exploration of new formulations to generate morphologies and heteroatom incorporated MCM-48 is the crucial step to achieve its extensive applications.

In the present work, V-MCM-48 samples with spherical morphology are synthesized by conventional hydrothermal method under low concentration of CTAB surfactant. The prepared materials exhibit high catalytic activities in the oxidation of styrene even at low temperature.

1 Experimental

1.1 Synthesis

In a typical synthetic procedure, the designed amount of NH_4VO_3 was first dissolved in 10 mL deionized water. 1.0125 g CTAB was dissolved in the mixed solvent composed of 69 mL deionized water, 6.3 mL ammonia solution (25%) and 32.4 mL EtOH (ethanol). Then the NH_4VO_3 solution and 2.1 mL tetraethylorthosilicate (TEOS) was slowly added into the above template solution under stirring. After being stirred for 2 hours, the synthesis gel was transferred into a polyethylene reactor and aged at 100 ℃ for 24 h. The sample was washed with deionized water and EtOH for several times, and then was dried at room temperature. The template was removed from the solid product by calcining at 550 ℃ in air for 6 h. The final material with molar ratio of 1TEOS/0.3CTAB/$n$$NH_4VO_3$/10$NH_3$/60EtOH/500$H_2O$ was noted as 100nV-MCM-48.

1.2 Characterization

The XRD patterns of all the synthesized materials were recorded on a Bruker AXS D8 Advance powder diffractometer using Ni filtered Cu $K\alpha$ (λ=0.154 178 nm) in the 2θ range of 1.5°~8.0°.

For SEM analysis, the samples were shadowed with gold, and then the surface microtopographies were taken with a Hitachi S4800 Field Emission Scanning Electron Microscopy.

N_2 adsorption-desorption isotherms were measured on a Micromeritics ASAP-2020 analyzer. Before the measurements, calcined samples were outgassed in vacuum at 300 ℃ for 5 h. Surface areas were calculated using the BET equation and pore size distributions were obtained by the Barrett-Joyner-Halenda (BJH) method using desorption branch data. The vanadium contents were analyzed using Jarrell-Ash 1100 Inductively Coupling Plasma spectrometer (ICP).

The FTIR spectra of the samples were recorded using Bruker VECTOR22 in KBr matrix in the range of 4 000~400 cm^{-1}.

The X-ray photoelectron spectrum (XPS) was conducted on PHI 5000 VersaProbe X-ray photoelectron spectrometer equipped with Al $K\alpha$ radiation (1 486.6 eV). The C1s peak at 284.6 eV was used as the reference for binding energies.

Laser Raman spectra (LRS) were recorded using a Renishaw In-vira microscopy Raman spectrometer, and an Ar^+ laser with an excitation wavelength 514.5 nm in a macromode.

51V MAS NMR experiments were performed with a 4.0 mm MAS probe on a Bruker Avance III spectrometer in a magnetic field strength of 9.4 T at a Larmor frequency of 105.181 MHz. Powdered samples were packed inside zirconia MAS rotors and spun at 14 kHz.

1.3 Catalytic test

Catalytic test was carried out in a two-necked flask. Typically, the catalyst (50 mg), acetonitrile (10 mL) and styrene (1.1 mL) were mixed. When temperature rose to 50 ℃, 1.5 mL of H_2O_2 was added into the reaction mixture. After reaction for 12 h, the catalyst was separated by centrifugation. The concentrations of the oxidation products were analyzed by a SP-6890 gas chromatograph (Lunan Ruihong Chemical Instrument Co. LTD, China) with 0.32 mm× 30 m SE-54 capillary column. Nitrogen was used as a carrier gas in the flow rate of 1.5 mL·min^{-1}, injection with a micro-syringe of 0.5 μL, column oven temperature 140 ℃, detection temperature and vaporization temperature both 260 ℃.

2 Results and discussion

2.1 Textural properties

Fig.1 shows the low-angle XRD patterns of the calcined MCM-48 samples with different vanadium contents. All the prepared samples exhibit a strong diffraction peak at $2\theta \approx 2.42°$ together with three small peaks at $2\theta \approx 2.8°$, 4.4° and 4.6°, which are indexed as (211), (220), (420) and (332), respectively. The XRD result confirms that the samples possess highly ordered three-dimensional cubic structure. The main (211) diffraction peaks for V-MCM-48 become broader and weaker with increase of vanadium content, indicating that the over-doping of vanadium species into the silica framework can cause low regularity of porous structure.

Fig.2 shows the N_2 adsorption-desorption isotherms and pore diameter distribution of V-MCM-48 samples. All the samples exhibit the typical IV type isotherm of mesoporous materials with a sharp jump in the relative pressure range of 0.25~0.35 and have narrow pore size distribution. It indicates all the samples have highly ordered porous structure. Several measured structural parameters of V-MCM-48 samples are listed in Table 1. It is clear that the unit cell parameter and pore diameter become higher with the increase in vanadium content, which suggests the incorporation of vanadium into the framework of silica

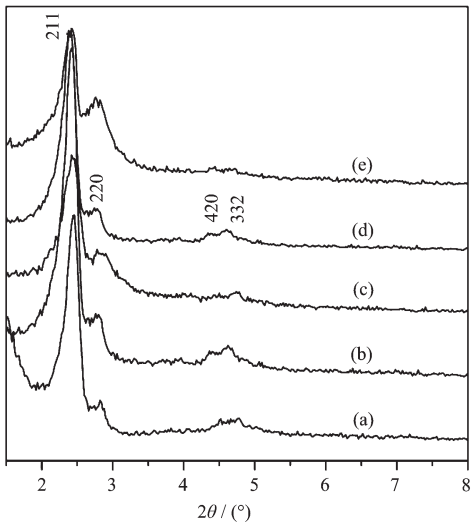

(a) Si-MCM-48; (b) 2V-MCM-48; (c) 4V-MCM-48; (d) 6V-MCM-48; (e) 8V-MCM-48

Fig.1 Low-angle XRD patterns for calcined MCM-48 samples with different vanadium contents

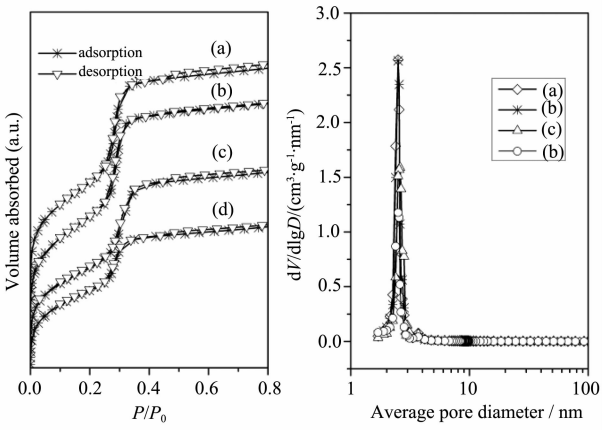

(a) 2V-MCM-48; (b) 4V-MCM-48; (c) 6V-MCM-48; (d) 8V-MCM-48

Fig.2 N_2 adsorption-desorption isotherms and pore diameter distribution of calcined V-MCM-48 samples

Table 1　Structural parameters of the samples with different vanadium contents

Catalyst	V/Si molar ratio[a] / %	d_{211} / nm	a_0 / nm	D[b] / nm	S_{BET} / ($m^2 \cdot g^{-1}$)	w_t[c] / nm
Si-MCM-48	—	3.59	8.79	2.38	1043	1.64
2V-MCM-48	1.15	3.65	8.94	2.50	996	1.64
4V-MCM-48	1.81	3.65	8.94	2.50	1005	1.62
6V-MCM-48	2.28	3.68	9.01	2.60	846	1.69
8V-MCM-48	2.91	3.71	9.09	2.5	750	1.65

[a] ICP results; [b] Pore diameter determined by BJH method from N_2 adsorption-desorption data; [c] w_t(wall thickness)=(a_0/3.091 9)−D/2.

due to the longer bond length of V-O bond [17]. BET surface areas of the samples decrease with the increase of vanadium content except 4V-MCM-48, possibly due to its spherical morphology (see Fig.3b). The reduction of surface area can be attributed to the lower regularity of pore structure caused by the incorporated of vanadium.

2.2　Morphology

The SEM images of the samples with different vanadium contents are shown in Fig.3. Three types of particles with different morphologies are observed.

The pH value of solution is between 10.6 and 11.3 in the synthetic process of spherical V-MCM-48. Under this condition, vanadium mainly exists in the form of HVO_4^{2-} at low vanadium concentration. With the increase of vanadium concentration, $V_2O_7^{4-}$ gradually becomes the dominant species[18-19].

A mechanism for the formation of spherical V-MCM-48 is suggested in Scheme 1. In the synthetic process of V-MCM-48, CTAB molecules firstly gather into small micelles (A) and they aggregate to cubic phase structure (B). Vanadium species exist as $V_2O_7^{4-}$ and HVO_4^{2-} under pH value of 10.6~11.3. HVO_4^{2-} with smaller ionic radius can distribute inside of the micelles (C) through the interaction of S^+I^- (where S^+ is the cation from the surfactant, I^- is the anion

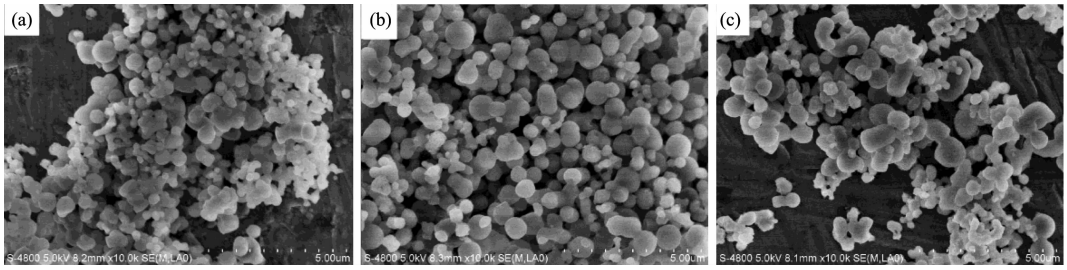

(a) 2V-MCM-48; (b) 4V-MCM-48; (c) 6V-MCM-48

Fig.3　SEM images of V-MCM-48 samples

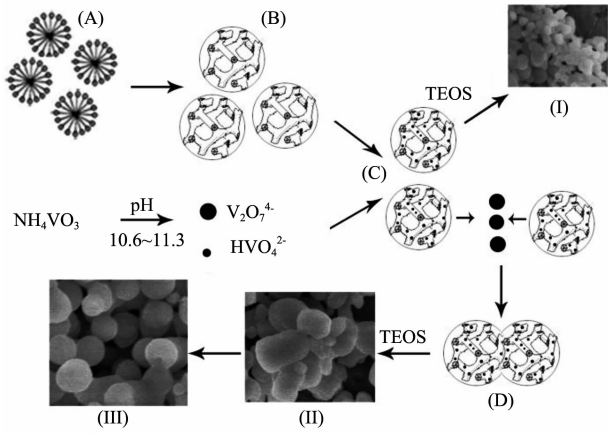

Scheme 1　Scheme for the formation of spherical V-MCM-48

from the salt). In contrast, $V_2O_7^{4-}$ with larger ionic radius cannot go into cubic phase structure (B), instead, $V_2O_7^{4-}$ is connected by several micelles (C) into larger elongated micelles (D) because of its strong electrostatic interaction with CTA^+.

TEOS, introduced into the solution, hydrolyzes to inorganic silica species. The silica species polymerize around the small micelles (C) and the elongated micelles (D), respectively, leading to the appearance of the small particles with particle size of ca. 200 nm ((Ⅰ) in scheme 1) and elongated particles ((Ⅲ) in scheme 1). After the gel is aged at 100 ℃ for 24 h, part of elongated particles (D) split into spherical particles with similar diameter 500~800 nm ((Ⅱ) in scheme 1). At the same time, the vanadium from HVO_4^{2-} is incorporated into the framework of silica.

HVO_4^{2-} species can hydrolyze simultaneously with the silica species and vanadium is incorporated into the framework of MCM-48. $V_2O_7^{4-}$ species are relatively stable under strong alkali condition. They remain in the solution instead of incorporating into the V-MCM-48 materials. Therefore, the vanadium content in the prepared material is relatively lower than that in the gel, especially when the V/Si molar ratio in the gel is higher (shown in Table 1).

2.3 States of vanadium

The IR spectra of the calcined V-MCM-48 samples are shown in Fig.4. The bands between 2 700 and 3 000 cm^{-1}, which reflect the existence of organic template (CTAB) [20], are not detected, indicating complete removal of surfactant from the matrix. The bands at 1 090 cm^{-1}, 800 cm^{-1} and 460 cm^{-1} are the symmetric and asymmetric stretching of Si-O-Si vibrations. The band around 1 633 cm^{-1} is attributed to the bending vibration of water molecules[21]. A weak peak at 960 cm^{-1} is observable for V-MCM-48 sample, which is attributed to Si-O-V band position. Therefore, the band in 960 cm^{-1} can be taken as a proof for the incorporation of vanadium atoms in the framework of V-MCM-48[22].

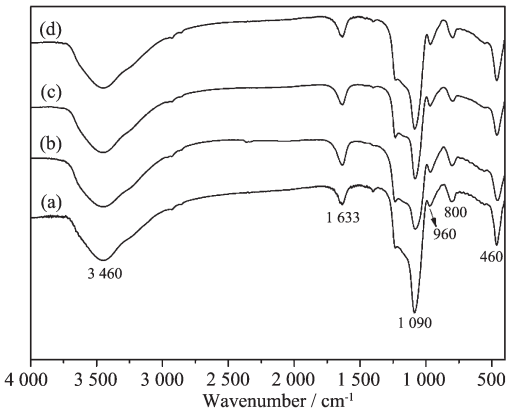

(a) 2V-MCM-48; (b) 4V-MCM-48; (c) 6V-MCM-48; (d) 8V-MCM-48

Fig.4 FTIR spectra of V-MCM-48 samples

Fig.5 shows the Laser Raman spectra of V-MCM-48 samples. The band at 1 030 cm^{-1} is assigned to the stretching vibration of short V=O bands of isolated distorted vanadium tetrahedron. The weak band at 920 cm^{-1} attributes to the silica vibration perturbed by the formation of V-O-Si band [23], suggesting the presence of vanadium species in the framework of MCM-48. This band intensifies with vanadium content increasing, supporting the arguement that the vanadium species are incorporated into the framework of MCM-48. For all the V-MCM-48 samples, the bands at about 994, 701, 525, 480, and 285 cm^{-1}, characteristic of crystalline V_2O_5, are not found[23-24].

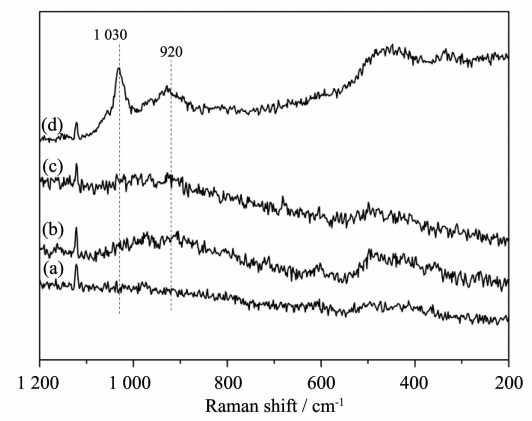

(a) 2V-MCM-48; (b) 4V-MCM-48; (c) 6V-MCM-48; (d) 8V-MCM-48

Fig.5 Raman spectra of V-MCM-48 samples

The ^{51}V MAS-NMR spectra of V-MCM-48 samples and V_2O_5 are presented in Fig.6. It is important to note that the ^{51}V MAS-NMR gives no indication of the presence of V_2O_5, which normally appears at −300 ppm. It is accordance to the Raman results. The signal at −576 ppm assigned to pentavalent vanadium in tetrahedral environment [25] is

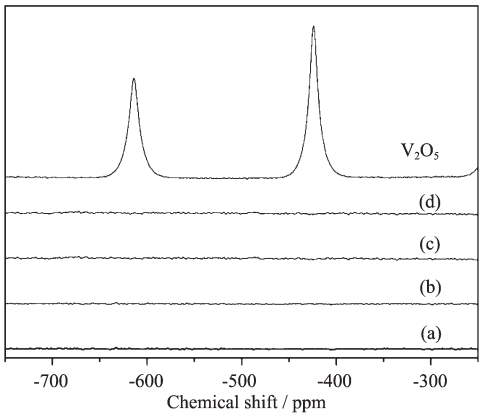

(a) 2V-MCM-48; (b) 4V-MCM-48; (c) 6V-MCM-48; (d) 8V-MCM-48

Fig.6　^{51}V MAS-NMR of V-MCM-48 samples

absence. It may be that the absence of chemical shift makes the signal not strong enough to be clearly observed.

Fig.7 presents V2$p_{2/3}$ XPS spectra of V-MCM-48 samples. The broad asymmetrical V2$p_{3/2}$ spectra can be de-convoluted into three components at 514.5 eV (assigned to V^{3+}), 516.2 eV (assigned to V^{4+}) and 517.4 eV (assigned to V^{5+}), respectively[26-27]. The V^{3+} species possibly are attributed to the reduction of V^{5+} or V^{4+} species. The peak at 517.4 eV is the largest, indicating that the V^{4+} species prevails in V-MCM-48 samples.

The vanadium loadings at the external surface of 2V-MCM-48, 4V-MCM-48, 6V-MCM-48 and 8V-MCM-48 are respectively 0.76%, 1.16%, 1.60%, 2.24%, lower than the corresponding value (1.15%, 1.81%, 2.28% and 2.91%) of V-MCM-48. It confirms that most of vanadium was doped to the framework of silica.

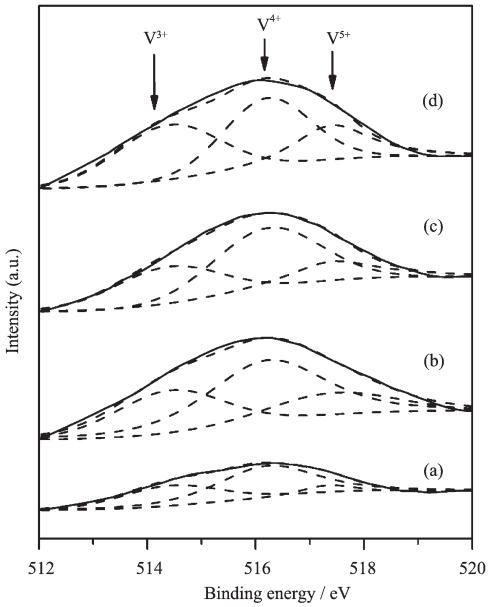

(a) 2V-MCM-48; (b) 4V-MCM-48; (c) 6V-MCM-48; (d) 8V-MCM-48

Fig.7　V2$p_{2/3}$ XPS spectra of V-MCM-48 samples

2.4　Oxidation of styrene with V-MCM-48

The data for the catalytic performance of V-MCM-48 in the oxidation of styrene are presented in Table 2. We can see that Si-MCM-48 displays a low styrene conversion. When V-MCM-48 is used as the catalyst, a high conversion of styrene (>70%) is obtained with benzaldehyde as the main product. It indicates that vanadium species in V-MCM-48 materials has a high catalytic activity for the oxidation of styrene. The conversion data indicates that the V^{4+} species in the framework are favorable for the increase in the catalyst activity of V-MCM-48. When vanadium content further increases to 2.91%, the conversion reduces slightly. It may be that excess V^{5+} species in

Table 2　Catalytic activity of V-MCM-48 and other catalysts in the oxidation of styrene

Catalyst	Conversion[a] / %	TON[b]	Selectivity / %				
			BZ[c]	PhA[d]	SO[e]	BA[f]	Others
Si-MCM-48	4	—	90	1	2	3	4
2V-MCM-48(1.15%)	74	759	91	2	0	2	5
4V-MCM-48(1.81%)	83	543	93	1	1	2	3
6V-MCM-48(2.28%)	90	473	90	1	2	2	5
8V-MCM-48(2.91%)	78	321	89	1	2	2	6

Note: [a]the conversion of styrene; [b]turn over number: moles of the substrate converted per mole metal, [c]the selectivity of Benzaldehyde; [d]the selectivity of Phenyl Acetaldehyde; [e]the selectivity of Styrene oxide, [f]the selectivity of Benzoic Acid

Reaction condition: Temperature 50 ℃, Styrene 1.1 mL, H_2O_2 1.5 mL, catalyst 50 mg, reaction time 12 h, acetonitrile 10 mL

8V-MCM-48 hinder the V^{4+} in the framework from contacting with the reactant to some extent. The lower regularity of mesoporous structure is an another reason for the reduction of conversion. The reaction mechanism can not be suggested clearly in the present work and needs to be further studied.

3 Conclusions

Highly ordered V-MCM-48 material was synthesized by one-step hydrothermal method using low CTAB template concentration. The V-MCM-48 prepared in this work has spherical morphology with a diameter of 0.5 ~1 μm as seen from SEM. Various characterizations show that most of vanadium is incorporated in the framework of V-MCM-48 materials. The V-MCM-48 materials show high conversion and selectivity to benzaldehyde in the oxidation of styrene at low temperature.

References:

[1] Beck J, V artuli J, Schmitt K, et al. *J. Am. Chem. Soc.*, **1992**,**114**(27):10834-10843

[2] Kresge C, Leonowicz M, Roth W, et al. *Nature*, **1992**,**359** (6397):710-712

[3] Lezanska M, Szymanski G S, Pietrzyk P, et al. *J. Phys. Chem. C*, **2007**,**111**(4):1830-1839

[4] Todorova S, Prvulescu V, Kadinov G, et al. *Micropor. Mesopor. Mater.*, **2008**,**113**:22-30

[5] KONG Yan(孔岩), ZHANG Rui(张瑞), XU Xin-Jie(徐鑫杰), et al. *Chinese J. Inorg. Chem.* (*Wuji Huaxue Xuebao*), **2008**,**24**(7): 87-292

[6] Alfredsson V, Anderson M W. *Chem. Mater.*, **1996**,**8** (5): 1141-1146

[7] Alfredsson V, Anderson M W, Ohsuna T, et al. *Chem. Mater.*, **1997**,**9**(10):2066-2070

[8] Solovyov L A, Belousov O V, Dinnebier R E, et al. *J. Phys. Chem. B*, **2005**,**109**(8):3233-3237

[9] Mathieu M, Voort P D, Weckhuysen B, et al. *J. Phys. Chem. B*, **2001**,**105**(17):3393-3399

[10]Kim T W, Chung P W, Lin S V. *Chem. Mater.*, **2010**,**22**: 5093-5104

[11]Matsumoto A, Tsutsumi K, Schumacher K, et al. *Langmuir*, **2002**,**18**(10):4014-4019

[12]Chanquia C M, Canepa A L, Sapag K, et al. *Top. Catal.*, **2011**,**54**(1/2/3/4):160-169

[13]Ide M, Wallaert E, Van D I, et al. *Micropor. Mesopo. Mater.*, **2011**,**142**(1):282-291

[14]Hu Y C, Wang J, Zhi Z Z, et al. *J. Colloid Interface Sci.*, **2011**,**363**(1):410-417

[15]Jiang L, Wang L Z, Zhang J L. *Chem. Commun.*, **2010**,**46** (42):8067-8069

[16]Petitto C, Galarneau A, Driole M F, et al. *Chem. Mater.*, **2005**,**17**(8):2120-2130

[17]Parvulescu V, Anastasescu C, Constantin C, et al. *Catal. Today*, **2003**,**78**(1/2/3/4):477-485

[18]Wehrli B, Stumm W. *Geochim. Cosmochim. Ac.*, **1989**,**53** (1):69-77

[19]Breit G N, Wanty R B. *Chem. Geol.*, **1991**,**91**(2):83-97

[20]Bukallah S B, Bumajdad A, Khalil K, et al. *Appl. Surf. Sci.*, **2010**,**256**(21):6179-6185

[21]Xu J, Chu W, Luo S. *J. Mol. Catal. A*: *Chem.*, **2006**,**256** (1/2):48-56

[22]Shylesh S, Singh A P. *J. Catal.*, **2004**,**228**(2):333-346

[23]Gao F, Zhang Y, Wan H, et al. *Micropor. Mesopor. Mater.*, **2008**,**110**(2/3):508-516

[24]Piumetti M, Bonelli B, Armandi M, et al. *Micropor. Mesopor. Mater.*, **2010**,**133**(1/2/3):36-44

[25]Selvam P, Dapurkar S. *Appl. Catal. A*: *Gen.*, **2004**,**276**(1/2): 257-265

[26]Guo B, Zhu L F, Hu X K, et al. *Catal. Sci. Technol.*, **2011**,**1** (6):1060-1067

[27]Wang C T, Chen M T, Lai D L. *Appl. Surf. Sci.*, **2011**,**257** (11):5109-5114